

$ABE$ , all of whose elements are parallel to the  $\vartheta = 0$  plane and have the slope  $2MA_2$ .

Experimental points will generally lie in the interior parts of the surface, while the quantities of interest, molecular length and extension, are

only obtainable from the boundary at  $c=0$ . A process of extrapolation is therefore necessary. Knowledge of the linearity of the surface at small values of  $c$  is important in performing the extrapolation properly.

THE JOURNAL OF CHEMICAL PHYSICS VOLUME 16, NUMBER 12 DECEMBER, 1948

## Apparatus and Methods for Measurement and Interpretation of the Angular Variation of Light Scattering; Preliminary Results on Polystyrene Solutions

BRUNO H. ZIMM

*Department of Chemistry, University of California, Berkeley 4, California*

(Received June 2, 1948)

A photoelectric apparatus for the measurement of the angular dependence of light scattering from solutions is described in detail and its performance is discussed. Methods of calculation for the determination of the average extension of the scattering molecules from the data are described. Data are presented for two fractions of polystyrene in various solvents, showing the effect of changing solvent power and temperature, and also confirming a theoretically derived formula for the concentration dependence of the scattering.

### I. INTRODUCTION

WHEN light is scattered from a macromolecule, such as a high polymer chain, an intensity distribution results which may be considered as a simple form of interference pattern. From appropriate measurements on the pattern the spatial extension of the molecule may be deduced.

The present paper describes new apparatus for obtaining the intensity distribution of the scattering. Several previous investigators<sup>1,2,3</sup> have also described apparatus for this purpose. The present equipment incorporates some important refinements over the previous types.

Theoretical developments, such as described by Debye<sup>4</sup> and by the author in the preceding paper,<sup>5</sup> are indispensable to the proper interpretation of the raw data. A method of application of the theory is therefore presented in some detail.

Finally, data on polystyrene solutions are

given. They seem to confirm the formulae derived in the preceding paper,<sup>5</sup> in addition to having physico-chemical interest of their own.

Although the average spatial extension of the molecules of a polymeric material affects most of its properties, light scattering from dilute solution seems to be the only way this dimension can be unambiguously determined. Approximate relative values can be found in some cases from viscosity measurements. For example, it has long been recognized that the "intrinsic viscosity" of a given polymer is smaller in thermodynamically poor solvents than in good ones, and this effect has been interpreted as indicating a curling up and contraction of the polymer chain in the unfavorable solvent.

An attempt has already been made to compare viscosity and light-scattering measurements of the solvent effect in polystyrene solutions.<sup>6</sup> The results were confusing in that a large change occurred in the viscosity but very little in the light scattering. The measurements have been repeated in part with the new apparatus and the earlier data have been found to be in error by a small but significant amount. In the new meas-

<sup>1</sup> R. S. Stein and P. M. Doty, *J. Am. Chem. Soc.* **68**, 159 (1946).

<sup>2</sup> P. P. Debye, *J. App. Phys.* **17**, 392 (1946).

<sup>3</sup> R. Speiser and B. A. Brice, *J. Opt. Soc. Am.* **36**, 364 (1946).

<sup>4</sup> P. Debye, *J. Phys. Coll. Chem.* **51**, 18 (1947).

<sup>5</sup> B. Zimm, *J. Chem. Phys.* **16**, 1093.

<sup>6</sup> P. Doty, W. Affens, and B. Zimm, *Trans. Faraday Soc.* **42B**, 66 (1946).

urements there is substantial agreement between the viscosity and light-scattering results.

Another effect of interest is the change of the spatial extension of the chains with temperature, since this is related to the relative energies of the different configurations the chain may assume. Some preliminary results on polystyrene are given.

## II. APPARATUS

The apparatus described here was built primarily to measure the intensity distribution of light scattered from dilute polymer solutions, the ultimate aim being to determine the extension of the molecules. In considering the design of such apparatus, the following general points may be kept in mind.

When a high polymer solution is illuminated by a beam of parallel and polarized light, the intensity of the scattered light varies smoothly with the angle of scattering. (A typical curve is shown in Fig. 6, curve *D*.) Except in the case of unusually large molecules, most of the variation occurs between the angles of  $30^\circ$  and  $150^\circ$ . The intensity of scattering is always small, of the same order of magnitude as the scattering from the solvent alone, since the solutions must be dilute to minimize intermolecular interferences. Dust specks in the solution are therefore a source of much trouble, especially at small angles where the large dust particles scatter most strongly. In consideration of the foregoing, it is not usually desirable to make measurements at angles close to the incident beam.

Experience has shown that freedom of the solution from foreign particles is the quality that limits the precision of measurement, provided the measuring apparatus itself can attain a precision of one percent or better.

The general specifications on an apparatus are therefore the following: (1) The apparatus should be capable of measurements of the relative intensity of scattering at angles from  $30^\circ$  to  $150^\circ$ , with a resolving power of about  $5^\circ$ ; (2) it should make these measurements on liquids whose turbidities are of the order of magnitude of those of the common organic solvents ( $10^{-4} \text{ cm}^{-1}$ ), with a precision of at least one percent.

As a primary detector of the scattered light, the recently developed multiplier phototube has important advantages. The output current of this tube is large enough to be measured with ordinary low-impedance equipment (less than 1 megohm), even when the light intensity is of the low order encountered in this investigation. In addition the response characteristic is stable and linear as long as the tube is not exposed to strong light.

To eliminate the effect of fluctuations in the light source, the intensity of the scattered light, as measured by the photomultiplier, may be compared to the intensity of a portion of the incident beam, measured by an ordinary vacuum photocell. The ratio of the currents is readily measured by passing them in opposite directions through a potentiometer.

A complication arises since the photomultiplier has a large dark current from the amplified thermionic emission of the photocathode. The difficulty was avoided by modulating the light at a definite frequency and phase and using only the components of that frequency and phase in the photocurrents. Further amplification is then easy using standard a.c. amplification techniques. Since a mercury arc lamp is naturally modulated at 120 c.p.s. when operated on an a.c. power line, this offers a very convenient way of eliminating the dark current.

### 1. General Plan

A block diagram of the apparatus is shown in Fig. 1.

The projector emits a beam of monochromatic light, modulated at 120 c.p.s., which passes

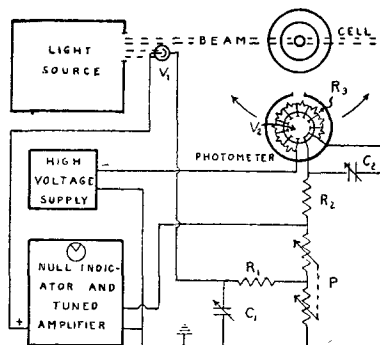


FIG. 1. Block diagram of apparatus.

$R_1, R_2$ , 0.1 megohm  
 $R_3$ , ten 50,000 ohm resistors in series  
 $C_1, C_2$ , 500  $\mu\text{f}$   
 $V_1$ , RCA 926  
 $V_2$ , RCA 931A

through the solution cell. A portion of the beam falls on the vacuum phototube  $V_1$ . Light scattered from the sample in the cell illuminates the sensitive photomultiplier tube  $V_2$ , which may be moved to receive light scattered at any desired angle.

The a.c. components of the currents from the two photo-cells are  $180^\circ$  out of phase because of the opposite polarity of the two cells. The currents are balanced in the precision potentiometer  $P$  by means of the tuned amplifier and electron-ray indicator. When the indicator shows a minimum, the setting of the potentiometer gives the ratio of the currents. The potentiometer readings are therefore proportional to the ratio of the scattered and incident intensities, which is the quantity desired.

The phase-shift networks  $R_1-C_1$  and  $R_2-C_2$  are used to sharpen the balance by compensating for the different capacities of the connecting wires.

The high negative voltage for the photomultiplier is supplied by a high voltage rectifier, while the positive voltage for the other phototube comes from a tap on the power supply of the electron-ray indicator.

## 2. The Light Source and Projector

A diagrammatic cross section of this part of the apparatus is shown in Fig. 2. The lamp,  $A$ , is a 100-watt medium-pressure mercury arc, General Electric Type AH-4. A pair of condensing lenses  $B$  forms an image of the lamp on the diaphragm  $D$ , thus providing an accessible secondary source whose size and shape may be easily adjusted. The filter  $C$  is included to isolate the desired wave-length. An image of the diaphragm  $D$  is produced in the middle of the solution cell  $J$  by the lens  $G$ .

Part of the beam is focused on the phototube  $V_1$  by the concave mirror  $F$ .<sup>7</sup> The remainder passes through a clear hole in the center of the mirror.

The plastic<sup>8</sup> prism  $H$  deviates the beam upward at an angle of eight degrees to compensate for the downward refraction suffered at the solution cell

<sup>7</sup> The mirror  $F$ , which does not require a good figure, was made simply by silvering an ordinary watch glass.

<sup>8</sup> The prism  $H$  was easily made with casting resin in a mold of microscope slides. The resin used was "Castolite" (The Castolite Company, Kenilworth, Illinois).

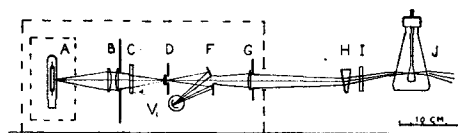


FIG. 2. Projector optical system.

$J$ . By removing the prism a horizontal beam for use with other types of cells is easily obtained.

$I$  is a "Polaroid" disk.

All elements are mounted on a sturdy optical bench and covered by a hood to contain stray light.

Over-all dimensions are indicated in the figure. The sizes of the important apertures are as follows: the lenses  $B$ , which serve as aperture stop for  $V_1$ , are 30 mm diameter; the opening in diaphragm  $D$ , serving as field stop of the system, is 6 mm (vertically) by 2 mm (horizontally); the aperture in  $F$ , which limits the aperture of the beam to the solution cell, is 15 mm (vertically) by 10 mm (horizontally). The maximum divergence of rays in this beam is about three degrees.

Some explanation of the design considerations may be useful at this point. It is desired to produce a beam of maximum intensity within the limits of the solution cell. The angular divergence of this beam is restricted also within specified limits (three degrees horizontally and five vertically in this case). Given the fixed dimensions of the lamp and solution cell, these conditions are to be achieved by the arrangement of the other elements of the system.

The positions of maximum illumination are images of the source. Therefore, an image of the lamp is focused in the solution cell  $J$ . The image is made larger than the cell and stopped down to the proper size by the diaphragm  $D$ , which also lies at an image of the lamp. In this way the cell is filled with a uniform illumination. The angular divergence is controlled by the aperture of lens  $G$ , which is actually determined by  $F$ .

The exact dimensions were determined by the materials and space available, within the limits specified by the above conditions.

## 3. The Solution Cell

The design and preparation of a suitable cell to hold the solution under investigation required more care than any other phase of this work.

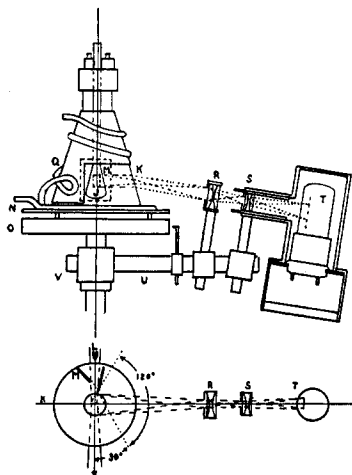


FIG. 3. Detail of solution cell and photometer.

Previous investigations have generally employed long rectangular cells with the beam traversing the long axis. In such a cell it is easy to eliminate stray light, but the volume of solution seen by the photometer changes with the angle of observation and the cell is large and wasteful of solution. Cylindrical cells have also been used, but in such cells multiple reflections of the incident beam occur and are very troublesome at angles other than those close to  $90^\circ$ .

The ideal cell would be small, compact and give by itself negligible scattering so that its whole volume could be observed by the photometer at all angles. It was found possible to approach this ideal by the arrangement shown in Fig. 3. The cell proper *J* is a thin-walled (0.2 mm) bulb of glass.<sup>9</sup> It is immersed in an outer vessel filled with a liquid of approximately the same refractive index as the solution in the bulb. The conical profiles of the bulb and outer vessel *K* are chosen to send reflections of the incident beam up or down out of the plane of the photometer, thus avoiding the principal defect of cylindrical cells. The thin walls of the bulb *J* are necessary to minimize scattering from the glass and foreign particles in it. Immersion in an outer liquid makes possible the small size without significant distortion of the light paths.

The illuminating light is confined to a narrow

<sup>9</sup> This bulb is made by heating a portion of a clean and scratch-free piece of 8 mm Pyrex tubing in a blast lamp until soft, then blowing and stretching in one operation an elongated bulb. One end of the bulb is then sealed off.

sharp-edged beam *L* which crosses the middle of the cell as shown in Fig. 3. The beam is unavoidably surrounded by a halo of diffuse light scattered from the front surface of the outer cell and preceding elements of the optical system. If this halo were allowed to strike the edges of the bulb *J*, reflections would result which would seriously interfere with measurements of forward scattering. To prevent this, blackened brass shields *M* are introduced, just outside the main beam, arranged as shown so that they do not interfere with the photometer at angles between  $30^\circ$  and  $150^\circ$ . At angles less than  $30^\circ$  some diffuse light from the edge of the shield *M* enters the photometer, although the amount is not serious except for the solutions of the lowest scattering power. As will be seen, measurements between  $30^\circ$  and  $150^\circ$  are adequate for most polymer solutions.

The outer vessel *K* is an ordinary 250 cc. Pyrex Erlenmeyer flask. Here, as in several other places in the optical system, it is unnecessary to have surfaces of high optical quality and very simple pieces of glassware may be used effectively. The outside of all parts of the flask *K* that do not have to transmit light are covered with black paint. The flask is cemented to a brass plate *N*. Three brass feet are brazed to the plate position of the assembly automatically by fitting into a set of grooves machined in the table *O*. The whole cell assembly is thus removable for cleaning and filling but can be replaced accurately and easily.

Partially surrounding *K* is a heavy copper jacket *Q* bearing a loop of copper tubing through which heating or cooling water may be passed. A loop of this coil is also soldered to the base plate *N*. Good thermal contact between the glass and copper was achieved by filling the space with typemetal.

The inner bulb *J* is held by a brass fitting with three adjustable jaws which rests on the top of the flask *K*. The top of the flask is squared off by grinding against a flat plate.

The liquid used to fill the flask should not be excessively volatile or corrosive, should have a refractive index close to that of the solution being studied, and should preferably have a low scattering power. Water, which has the lowest scattering power of any of the common liquids, becomes turbid rapidly from microorganisms and is not suitable on this account. 1-propanol,

$n_D = 1.37$ , has a relatively low scattering power and makes a substitute for water. Other liquids found suitable are toluene,  $n_D = 1.50$ , and 1,2-dichloroethane,  $n_D = 1.44$ . The latter two unfortunately have rather high scattering powers. In any case, it is necessary to clean the liquids carefully to exclude dust.

#### 4. The Photometer

The photometer assembly is also included in Fig. 3.

Scattered light from the cell is received by the objective lens  $R$  and an image of the cell is focused on the diaphragm at  $S$ . The lens  $S$  forms an image of the diaphragm  $R$  on the cathode of the photomultiplier tube  $T$ . The diaphragm at  $S$  serves as the field stop of the photometer, excluding stray light arising in other parts of the optical system, such as especially the places where the beam enters and leaves the flask  $K$  and reflections of these spots from the walls. The diaphragm at  $R$ , which measures  $3 \times 10$  mm, is the aperture stop of the system. Its image on the photocathode  $T$  remains constant in size, shape, and uniformity of illumination as the photometer is moved. Since the photocathode varies in sensitivity over its surface, this constancy is an important consideration.<sup>10</sup>

The phototube is totally enclosed by a brass housing as shown. A cap may be placed over the opening at  $S$  to protect the tube from daylight. A compartment also encloses the tube socket and the ten 50,000 ohm resistors which are soldered to it. The tube and its housing may be conveniently removed from the rest of the assembly so that the optical system may be adjusted.

The whole photometer assembly is adjustably mounted on the rod  $U$ , which revolves around the central support of the cell assembly on a bearing at  $V$ . A graduated scale on the rim of the table  $O$  and a pointer on  $U$  show the angle of observation.

#### 5. Power Supply

The two milliamperes at 600–900 volts for the photomultiplier tube are supplied by the regulated rectifier shown in Fig. 4. Since this is an

<sup>10</sup> It was first attempted to focus the image of the cell directly on the photocathode, but it was soon found that the response of the tube varied by fifty percent when the image changed its shape during the revolution of the photometer about the solution bulb.

adaptation of a well-known circuit, it will not be described completely. Regulation is accomplished by a degenerative pentode circuit, actuated by the variation of the output voltage with respect to a standard potential supplied by the "B" battery.

The resistor  $R_2$  is included to provide negative feedback and diminish the effects of drift in the characteristics of the control tube  $V_5$ , which seems to be the main source of instability. Negative feedback would normally reduce the efficiency of regulation, but a compensating over-regulating effect is introduced by connecting the screen grid of  $V_5$  to a tap on the unregulated input voltage. Selection by trial of the proper feedback resistance leads to almost perfect cancellation of these two effects.

It was found desirable to place the "B" battery at some distance from the regulator in an enclosed cupboard to protect it from rapid temperature variations. Another source of instability was eliminated by the use of wire-wound resistors in the voltage control network, as specified in Fig. 4.

The small residual drift occurs mainly in the

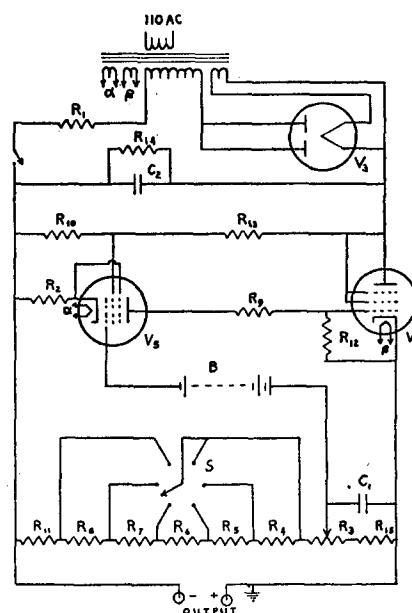


FIG. 4. Regulated high voltage supply.

$R_1$ , 1500 ohms	$R_{14}$ , 1 megohm
$R_2$ , 6000 ohms wirewound	$R_{15}$ , 1 megohm wirewound
$R_3$ – $R_8$ , 10,000 ohms wirewound	$C_1$ , 0.01 $\mu$ f
$R_9$ , 25,000 ohms	$C_2$ , 2 $\mu$ f
$R_{10}$ , 50,000 ohms	$V_3$ , 80
$R_{11}$ , 140,000 ohms wirewound	$V_4$ , 6AG7
$R_{12}$ , 250,000 ohms	$V_5$ , 6J7
$R_{13}$ , 500,000 ohms	$B$ , 90 volt "B" battery

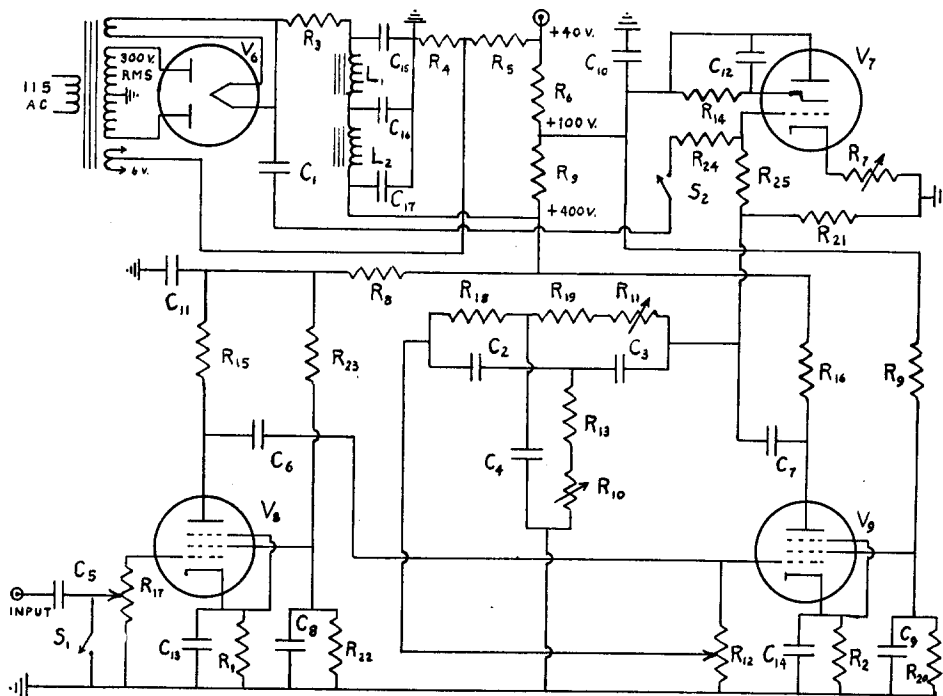


FIG. 5. Narrow-band amplifier and electron-ray indicator.

$R_1, R_2$ , 2250 ohms	$C_1$ , 250 $\mu\text{f}$
$R_3, R_4$ , 5000 ohms	$C_2, C_3$ , 2500 $\mu\text{f}$
$R_5, R_6$ , 20,000 ohms	$C_4$ , 5000 $\mu\text{f}$
$R_7, R_8$ , 50,000 ohms	$C_5, C_6, C_7$ , 0.01 $\mu\text{f}$
$R_9, R_{10}, R_{11}$ , 0.1 megohm	$C_8, C_9$ , 0.05 $\mu\text{f}$
$R_{12}, R_{13}$ , 0.25 megohm	$C_{10}$ , 0.1 $\mu\text{f}$
$R_{14}-R_{15}$ , 0.5 megohm	$C_{11}$ , 0.25 $\mu\text{f}$
$R_{19}$ , 0.75 megohm	$C_{12}$ , 2 $\mu\text{f}$
$R_{20}-R_{22}$ , 1 megohm	$C_{13}-C_{17}$ , 8 $\mu\text{f}$
$R_{23}$ , 3 megohm	$L_1, L_2$ , 15 h
$R_{24}$ , 5 megohm	$V_6$ , 80
$R_{25}$ , 10 megohm	$V_7$ , 6E5
	$V_8, V_9$ , 6J7

first two hours after the current is turned on. During this time the voltage variations cause a change in the sensitivity of the photomultiplier of about five percent. Thereafter, the drift is slow and not a serious hindrance to measurements. It is usually less than one percent per day.

The inclusion of manual control ( $R_3$  and  $S$ ) of the output voltage so the phototube may be set at any desired sensitivity has proven to be most useful.

## 6. Tuned Amplifier and Electron-Ray Indicator

As explained previously, measurement consists of adjusting the potentiometer  $P$  of Fig. 1 until the 120 cycle component of the voltage across it reaches a minimum. To observe this voltage the tuned amplifier diagrammed in Fig. 5 was constructed.

Essentially the amplifier is a two-stage resistance-capacity-coupled high gain voltage amplifier with a frequency dependent feedback network added to the second stage. Except for the latter, the construction is entirely conventional, the circuit constants those recommended by the tube manufacturer.<sup>11</sup> Careful shielding of the input stage is necessary.

The feedback network is the "twin-T" type. It was adjusted, with the temporary aid of an oscilloscope, essentially in the manner described by Sturtevant,<sup>12</sup> to supply regeneration at 120 c.p.s. and degeneration at other frequencies. The amount of feedback, which is controlled by the potentiometer  $R_{12}$ , is usually adjusted so that the amplifier is just short of oscillation and so that

<sup>11</sup> *Receiving Tube Manual* (RCA Manufacturing Company, Inc.).

<sup>12</sup> J. M. Sturtevant, *Rev. Sci. Inst.* **18**, 124 (1947).

the response time of the amplifier is about 0.5 second ( $Q \sim 300$ ). The use of a remote cut-off tube in this stage with a small (0.25 megohm) resistance in the grid circuit was found to give smoother control of the regeneration than more conventional arrangements.

It is necessary to use a narrow-band amplifier such as described here since the noise level in the highly amplified photocurrent is unusually high.

The output of the amplifier is detected by the electron-ray ("magic eye") tube  $V_7$ . In operation the bias control  $R_7$  is set so that the tube is near cut-off and the eye is just closed when the input of the amplifier is short-circuited by switch  $S_1$ . A signal then causes the eye to open. A signal of about  $10^{-5}$  volt causes a perceptible response at full gain. The capacitor  $C_{12}$  on the ray control electrode raises the response time of the tube to one second, enabling it to integrate over more rapid fluctuations in the photocurrent.

To aid in trimming the frequency of the feedback network, which drifts slightly, a standard 120 c.p.s. signal from the power supply may be imposed on the grid of the electron-ray tube by closing the switch  $S_2$ . The beats between this signal and the self-oscillations of the amplifier may then be observed. The frequency of oscillation is adjusted by trimming  $R_{19}$ .  $R_{25}$  isolates the oscillations from the test signal voltage.

When the utmost precision is desired, it is advantageous to study the output of the amplifier on an oscilloscope, observing the phase as well as the amplitude of the voltage as the measuring potentiometer ( $P$  in Fig. 1) is balanced.

### 7. General Construction

The potentiometer  $P$  of Fig. 1 was constructed by ganging together the corresponding dials of two 99,990 ohm decade boxes in such a way that the sum of the resistances of the two remains constant at 99,990 ohms while the ratios vary from 0 to  $\infty$ .

The whole apparatus was mounted on a table which was covered by a grounded aluminum sheet. Shielded cable was used in all exposed wiring, and all metal parts not otherwise connected were grounded. These precautions reduced interfering voltages from the power lines, etc., to a satisfactory level.

No attempt was made to enclose the apparatus

in a light-excluding case. Instead the room was darkened while measurements were made. A red light was used for illuminating the scale, recording data, and general manipulation (the photomultiplier being relatively insensitive to red). The principal consideration in this procedure was the desire always to have the cell open to visual inspection, to detect misalignment or dust, or suspended matter in the solutions under observation.

### 8. Performance

The performance of the photomultiplier tube, which is the heart of the apparatus, was in accord with that described by other authors.<sup>13</sup> Relevant to this work are the fatigue, dark current, and linearity characteristics of the device. There is great variation among individual tubes. The following remarks apply only to the better ones tested.

Fatigue was found to be negligible as long as the output was limited to five  $\mu a$ . At higher currents fatigue was noticeable. The potentiometer arrangement used limits the photomultiplier current to less than the balance tube current, which is approximately two  $\mu a$ . Fatigue is therefore not important.

Linearity was tested by measuring the transmission of a screen of 35.6 percent transmission over the usable range of light intensities. No deviation within the precision of measurement could be found.

The dark current of the tube used was found to vary from 0.005 to 0.05  $\mu a$ , depending on the voltage. With a total voltage of 800 volts the current was 0.01  $\mu a$  and the fluctuations were of the order of  $10^{-4}$   $\mu a$  per second. This would correspond to the amplified statistical fluctuation of a thermionic emission of about  $10^5$  electrons per second plus the spontaneous fluctuations of the multiplying stages. For comparison, the photocurrent from a cell full of butanone, the measurement of lowest intensity encountered, was approximately 0.01  $\mu a$  at this voltage. Statistical fluctuations in the photocurrent are also of the order of  $10^{-4}$   $\mu a$  per second, so that the over-all

<sup>13</sup> R. W. Engstrom, J. Opt. Soc. Am. **37**, 420 (1947); Fitz-Hugh Marshall, J. W. Coltman, and L. P. Hunter, Rev. Sci. Inst. **18**, 504 (1947).

TABLE I. Relative intensity of scattering from cell containing butanone.

Angle	Intensity
25.8°	6.78
36.9°	2.22
53.0°	1.29
66.4°	0.81
78.4°	0.58
90.0°	0.47
101.6°	0.41
113.6°	0.47
126.9°	0.54
143.1°	0.66

precision of the measurement is limited to about 1.5 percent.

At higher light intensities the fluctuation of the dark current becomes negligible, but the fluctuations of the photocurrent persist, varying as the square root of the intensity. In fact, the limit of precision is set by these fluctuations. The size of the fluctuations may be diminished by increasing the rise time of the amplifier. Since they decrease only as the square root of the time, while the tedium of measurement increases at least directly with the time, it is not usually desirable to increase the latter beyond one second, however. Probably the best procedure is to increase the power of the light source.

The stability of the photo-multiplier itself, as long as it was not exposed to strong light, apparently was limited only by the stability of its power supply. After having been run for several hours, the slow drift of the latter produced a variation of sensitivity of about one percent per day. It was necessary in accurate work to adjust the voltage occasionally by measuring the scattering of a standard of known scattering power.

The reading of the whole device was nearly independent of the fluctuations in the intensity of the light source, changing about one percent when the latter changed by a factor or two. The cause of this remaining change may have been that the light falling on the two phototubes did not come from exactly the same part of the source in each case.

It was generally found possible to make reproducible readings with a precision of 0.2 percent, when the statistical fluctuations of the electron current allowed, if a standard were measured within fifteen minutes of the reading.

The performance of the photometer in measuring the true angular variation of intensity of the scattered light was checked by measuring the fluorescence of a dilute solution of fluorescein (in water) or diacetylfluorescein (in toluene or dichloroethane). The solutions were illuminated with the blue lines of the mercury lamp while a yellow filter, opaque to the exciting light but transparent to the green fluorescence, was placed in front of the photometer. The solutions were dilute enough so that loss of light by absorption was negligible. Under these conditions the only causes of angular dissymmetry must lie in the geometry of the apparatus. It was found that there was a diminution of intensity at 90° of about three percent compared to 30° or 150°. Such a variation is to be expected, since the cell is not an ideal point source. The observed variation was used to correct subsequent measurements of scattering for this factor.

As an example of the intensity of the background and stray illumination when scattering (not fluorescence) was being measured, Table I is given. In this case the cell contained clean butanone and the outer vessel clean 1-propanol. The light observed at 90° is mainly the scattering of the butanone in the cell. The principal increase at larger and smaller angles occurs as larger volumes of the illuminated portion of the outer liquid contribute their scattering, while at the small angles scattering from imperfections in the cell walls and from the edges of the shields becomes important. The practical limit is reached at 10°, where the scattering from the spot at which the beam enters the outer vessel first comes into the photometer.

As pointed out above, an object of constant scattering power is needed as a reference in accurate work. After some experimentation, a rectangular block was made of polystyrene to which five percent of methyl acrylate had been added when the polymerization was half completed. The addition of the acrylate produced a copolymer of somewhat different internal pressure in the latter half of the polymerization. The mixture shows the opalescence expected from a one-phase liquid mixture near the consolute point. (Too much acrylate causes the separation of a second phase.) This block has served its purpose well, but its turbidity varies with temperature so that



it is desirable to keep it thermostated. A less sensitive material would be desirable.

As concrete examples of the results obtained, the curves of Fig. 6 are shown. The solid lines are the polar plot of the experimental intensity of scattering from a monodisperse sulfur sol, prepared according to the method of Johnson and LaMer.<sup>14</sup> Such a sol consists of spherical drops of liquid sulfur suspended in water. The maxima and minima, which may be considered as resulting from interference effects, are clearly shown. Comparison with Johnson and LaMer's results places the radius of these particles at 0.45 micron. The incident light here, as in all the other angular variation measurements, was polarized perpendicularly to the plane of measurement.

The dotted line in Fig. 6 is the scattering from a sample of polystyrene, to which reference will be made later in Section IV 1, dissolved in toluene to the concentration of 0.0002 g per ml. The "blank" obtained from the cell full of pure toluene has been subtracted from these measurements so that the curve represents the excess of scattering of the solution beyond that of the solvent. The curve itself is the plot of the theoretical equation, Eq. (1), while the circles are the experimental points. While the region between 25° and 150° only is readily accessible experimentally at low scattering intensities, it may be noted that most of the variation occurs within this range. This fortunate fact holds true even more strongly for polymers of smaller size.

It should finally be pointed out that the graph of the scattering from a suspension of ideally small particles would be a circle centered on the origin, such as the coordinate circles in Fig. 6.

### III. METHOD OF HANDLING DATA

It was shown by the theoretical treatment of the preceding paper<sup>5</sup> that at low concentrations the intensity of scattering,  $I$ , is related most simply to the concentration,  $c$ , and angle,  $\vartheta$ , by the equation

$$K(c/I) = 1/MP(\vartheta) + 2A_2c, \quad (1)$$

where  $P(\vartheta)$  is a known function of  $\vartheta$ ,  $M$  is the solute molecular weight, and  $A_2$  and  $K$  are constants. It may be anticipated that there will be

<sup>14</sup> I. Johnson and V. K. LaMer, J. Am. Chem. Soc. 69, 1184 (1947).

deviations from this equation if either the molecular weight or the concentration becomes too high. Nevertheless, it should be useful as a rough guide even in the latter case.

It is usually desired to obtain  $M$ , the molecular weight of the polymer, and  $P(\vartheta)$ , from which the average spatial extension of the chain may be calculated. Obviously these quantities can only be found by extrapolation of the experimental values of  $c/I$  to infinite dilution.

### 1. Some Properties of $P(\vartheta)$

Assuming for the moment that the extrapolation to infinite dilution may be accomplished, let us consider the function  $P(\vartheta)$ .

For a suspension of linear coiling chain molecules of uniform degree of polymerization,  $n$ , with light of wave-length  $\lambda$ ,  $P(\vartheta)$  is given by

$$P(\vartheta) = (2/u^2)(e^{-u} - 1 + u), \quad (2)$$

where

$$u = (8\pi^2 b^2 n / 3\lambda^2) \sin^2(\vartheta/2) = Cb^2 n \sin^2(\vartheta/2). \quad (3)$$

The constant  $b$  has the dimensions of length. It is determined by the average size and geometric arrangement of the bonds of the chain skeleton (see Eq. (20) below). The root-mean-square end-to-end chain distance,  $L$ , which is often employed, is equal to  $b^2 n$ .

To find the characteristic length,  $b$  (or  $L$ ), from the observed  $P(\vartheta)$ , it is convenient to enlarge on some observations by Debye.<sup>4</sup> If  $P(\vartheta)$  is expanded in terms of  $\sin^2(\vartheta/2)$ , the following series results:

$$P(\vartheta) = 1 - (C/3)nb^2 \sin^2(\vartheta/2) + (C^2/12)n^2b^4 \sin^4(\vartheta/2) - \dots \quad (4)$$

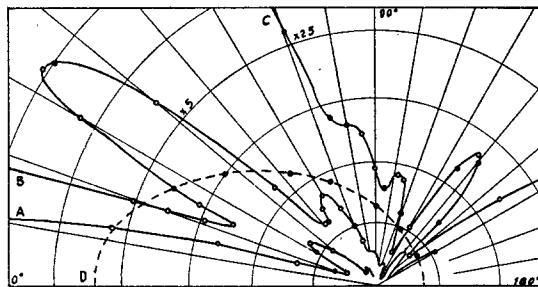


FIG. 6. Typical scattering curves, polar plots of intensity of scattering against angle of scattering. A, Sulfur sol of 0.45 microns radius in water; B, curve A times five; C, curve A times 25; D, excess scattering from polystyrene RT-H in toluene, concentration 0.0002 g/ml. (Radius vectors in arbitrary units.)

It is apparent that  $b$  may be found from the initial slope of the curve. Diminished curvature results if the reciprocal of  $P(\vartheta)$  is taken,

$$P^{-1}(\vartheta) = 1 + (C/3)nb^2 \sin^2(\vartheta/2) + (C^2/36)n^2b^4 \sin^4(\vartheta/2) - \dots \quad (5)$$

The characteristic length,  $b$ , is then easily found if the initial slope of the plot of  $1/P(\vartheta)$  against  $\sin^2(\vartheta/2)$  can be determined.<sup>15</sup> Fortunately such a plot already results if Eq. (1) is used to extrapolate the observations to infinite dilution.

When  $u = Cb^2n \sin^2(\vartheta/2)$  is less than unity  $P^{-1}(\vartheta)$  is practically linear in  $\sin^2(\vartheta/2)$  and there is no difficulty in obtaining the initial slope. But when  $u$  is larger than unity, the plot shows a gentle upward curvature and it is not always easy to find the initial slope directly.

A plot of  $P^{-1}(\vartheta)$  against  $u$  is shown in Fig. 7 (curve of  $z = \infty$ ) together with its initial slope and its asymptote for large values of  $u$ . The asymptote may be seen from (2) to be

$$\lim_{u \rightarrow \infty} P^{-1}(\vartheta) = (u + 1)/2. \quad (6)$$

Equation (6) is a line of intercept  $\frac{1}{2}$  and slope  $\frac{1}{2}$ , while the initial slope of  $P^{-1}(\vartheta)$  is  $\frac{1}{3}$  and the intercept is 1. It is obvious that data falling on any limited portion of the curve could be mistakenly thought to determine a straight line whose intercept and slope would not agree with

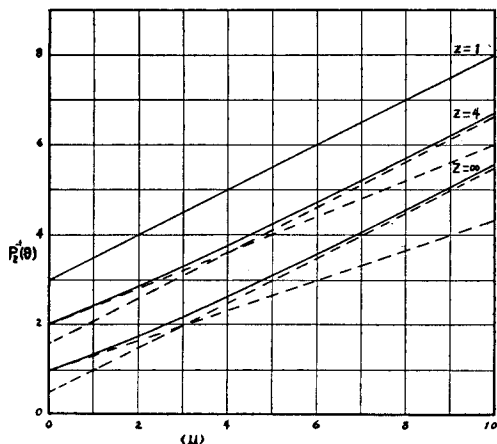


FIG. 7.  $P_s^{-1}(\vartheta)$  plotted against  $u = (8\pi^2(n)b^2/3\lambda^2)\sin^2(\vartheta/2)$  for three values of  $z$ . The curve for  $z = 4$  is displaced upward one unit and that for  $z = 1$  two units.

<sup>15</sup> As Debye points out, the initial slope gives in general the moment of inertia of the particle about its center of mass, regardless of the shape of the particle.

the true intercept and initial slope. A correction table, to be described, is useful in such a case.

When the particles under observation have other shapes than random coils, similar methods may still be used, although the forms of the equations are different. For example, if the particles are rigid linear rods of length  $L$ ,  $P(\vartheta)$  is given by

$$P(\vartheta) = \frac{1}{x} \int_0^{2x} \frac{\sin v}{v} dv - \left(\frac{\sin x}{x}\right)^2, \quad (7)$$

where  $x$  is given by

$$x = (2\pi L/\lambda) \sin(\vartheta/2). \quad (8)$$

In this case  $P^{-1}(\vartheta)$  may be expanded in  $x^2$  to give the form analogous to Eq. (5);

$$P^{-1}(\vartheta) = 1 + x^2/9 + 7x^4/2025 + \dots \quad (9)$$

The asymptote of  $P^{-1}(\vartheta)$ , analogous to Eq. (6), is

$$\lim_{z \rightarrow \infty} P^{-1}(\vartheta) = 2/\pi^2 + 2x/\pi. \quad (10)$$

### 2. Polydispersity

Further complications arise if the solute exhibits a distribution of degrees of polymerization, as is usually the case in practice. Let us assume that instead of only one degree of polymerization,  $n$ , there is a distribution,  $f(n)$ , such that  $f(n)dn$  is the weight fraction of material of degree  $n$  in the range  $dn$ . At infinite dilution, the total light scattering will be the sum of the scattering from each of the individual components. From Eq. (13b) of the previous paper,<sup>5</sup> the total scattering may then be found to be:

$$I(\vartheta)/c = K' \int n f(n) P(\vartheta) dn, \quad (11)$$

where  $K' = nk/M$  is a constant independent of  $n$ .

Considering now only the situation in the case of coiling solute particles, let us first examine it for small values of  $u = Cb^2n \sin^2(\vartheta/2)$ . If  $P(\vartheta)$  is expanded as in Eq. (4), and then integrated according to (7), the following series eventually results:

$$\frac{c}{I(\vartheta)} = \frac{1}{K' \langle n \rangle} \left[ 1 + \langle n \rangle \left( 1 + \frac{\langle \Delta n^2 \rangle}{\langle n \rangle^2} \right) \times \frac{Cb^2}{3} \frac{\vartheta}{2} \sin^2 \frac{\vartheta}{2} + \dots \right], \quad (12)$$

where

$$\langle n \rangle = \int n f(n) dn,$$

and

$$\langle \Delta n^2 \rangle = \int (n - \langle n \rangle)^2 f(n) dn.$$

The quantity  $\langle n \rangle$  is the weight-average degree of polymerization and  $\langle \Delta n^2 \rangle$  is the dispersion of the distribution. It is interesting that the quantity  $\langle n \rangle (1 + \langle \Delta n^2 \rangle / \langle n \rangle^2) = \langle n^2 \rangle / \langle n \rangle$  is the kind of average degree of polymerization which has been called the "Z-average" by writers on the theory of the ultracentrifuge.<sup>16</sup>

Comparing (12) with (1) and (5) leads to interesting conclusions. The molecular weight obtained from the extrapolation to zero angle is the weight-average molecular weight, but the average entering the slope from which the characteristic length is determined is the "Z-average," which is always larger than the weight average. If the dispersion,  $\langle \Delta n^2 \rangle$ , of the distribution can be found, one can be calculated from the other.

For large values of average  $u$ ,

$$\langle u \rangle = C b^2 \langle n \rangle \sin^2(\vartheta/2),$$

Eq. (12) converges slowly and it is difficult to determine the initial slope. We will therefore develop a special method which will sometimes be useful in such cases.

For many materials, it will be possible to approximate the distribution  $f(n)$  by a function of

TABLE II.

$z = \infty$			$z = 4$			$z = 19$		
$u$	$P^{-1}(\vartheta)$	Limiting tangent Ratio	$u$	$P^{-1}(\vartheta)$	Limiting tangent Ratio	$u$	$P^{-1}(\vartheta)$	Limiting tangent Ratio
0	1.00	1.00	0	1.00	1.00	0	1.00	1.00
1	1.36	1.33	1	1.42	1.40	1	1.37	1.35
2	1.76	1.67	2	1.86	1.80	2	1.70	1.70
3	2.19	2.00	3	2.32	2.20	3	2.22	2.05
4	2.65	2.33	4	2.78	2.60	4	2.68	2.40
5	3.12	2.67	5	3.27	3.00	5	3.15	2.75
6	3.60	3.00	6	3.75	3.40	6	3.63	3.10
7	4.08	3.33	7	4.23	3.80	7	4.61	3.80
8	4.57	3.67	8	4.72	4.20	8	5.59	4.60
9	5.07	4.00	9	5.20	4.60	∞	—	—
10	5.56	4.33	10	5.71	5.00	∞	—	0.70
∞	—	—	∞	—	—	∞	—	0.80

the form

$$f(n) = (y^{z+1}/z!) n^z e^{-yn}, \tag{13}$$

where  $y$  and  $z$  are adjustable parameters. This is a function with a single peak whose width is determined by the parameter  $z$ . By integrating the function, we find

$$\int f(n) dn = 1, \tag{14a}$$

$$z = (\langle n \rangle^2 / \langle \Delta n^2 \rangle) - 1, \tag{14b}$$

and

$$y = \langle n \rangle / \langle \Delta n^2 \rangle = (z + 1) / \langle n \rangle. \tag{14c}$$

The distribution is therefore characterized by the average degree of polymerization and its dispersion.

The advantage of this function for the present problem lies in the fact that the integration in Eq. (11) may be performed easily. When it is applied to the calculation of  $c/I(\vartheta)$ , the result is

$$\frac{c}{I(\vartheta)} = \frac{C^2 b^4 \langle n \rangle \sin^4 \vartheta / 2}{2K'} \left\{ \frac{z(1+z+C b^2 \langle n \rangle \sin^2 \vartheta / 2)^z}{(1+z)^{1+z} - (1+z - z C b^2 \langle n \rangle \sin^2 \vartheta / 2)(1+z+C b^2 \langle n \rangle \sin^2 \vartheta / 2)^z} \right\}, \tag{15}$$

$$= (1/K' \langle n \rangle) P_z^{-1}(\vartheta).$$

The new function,  $P_z^{-1}(\vartheta)$ , is plotted in Fig. 7 for  $z=4$  (dispersion,  $\langle \Delta n^2 \rangle$ , equal to  $0.20 \langle n \rangle^2$ ) and  $z=1$  ( $\langle \Delta n^2 \rangle = 0.50 \langle n \rangle^2$ ), in addition to the plot of the reciprocal of Eq. (2), to which  $P_z(\vartheta)$  reduces when  $z$  approaches infinity (dispersion approaches zero).

The case where  $z=1$  is of special interest,<sup>17</sup> since here the distribution of sizes,  $f(n)$ , is just

<sup>16</sup> Svedberg and Petersen, *The Ultracentrifuge* (Oxford University Press, Oxford, 1940).

<sup>17</sup> I am greatly indebted to Professor Debye for pointing this out to me.

that expected in certain types of polymerization.<sup>18</sup> Examination of Eq. (15) shows that here also  $P_z^{-1}(\vartheta)$  assumes an especially simple form:

$$P_1^{-1}(\vartheta) = 1 + C b^2 \langle n \rangle \sin^2(\vartheta/2) / 2. \tag{16}$$

In this case obviously the characteristic length  $b$  may be found easily from a linear plot of  $c/I(\vartheta)$  against  $\sin^2(\vartheta/2)$ .

In general, Eq. (15), with the use of Eq. (14b), approaches the linear form (12) as  $\langle u \rangle$  approaches

<sup>18</sup> P. J. Flory, *Chem. Rev.* **39**, 137 (1946).

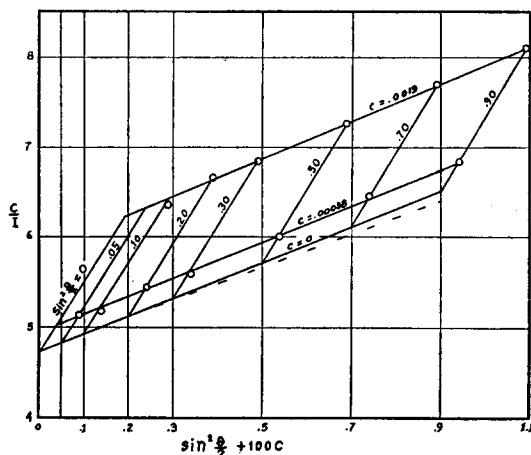


FIG. 8. Projection of the reciprocal intensity surface of polystyrene EP-2 in butanone at 67°C. The dotted line is the limiting tangent.

zero, and as  $\langle u \rangle$  becomes infinite Eq. (15) moves toward the line,

$$\frac{c}{I(\vartheta)} = \frac{1}{K'\langle n \rangle} \left[ \frac{z+1}{2z} + \frac{Cb^2\langle n \rangle \sin^2(\vartheta/2)}{2} \right], \quad (17)$$

as an asymptote. These limiting lines are also shown in Fig. 7. It can be seen that they come closer as  $z$  decreases until they fuse at  $z=1$  into one line.

Except when  $z=1$ , the curvature of  $c/I(\vartheta)$  may add difficulties to the determination of the characteristic length,  $b$ , from experimental data, as mentioned before. Table II has been prepared to facilitate the process. In the second column of each section is given  $P_z^{-1}(\vartheta)$ , in the third column the value of the corresponding limiting form (12). The ratio of the two quantities is given in the fourth column. By the use of the ratio, data falling on the curve may be reduced to the limiting line, from which  $b$  is easily found. Examples are given in Section IV, 4.

It remains to find  $\langle \Delta n^2 \rangle$ , the dispersion of the distribution. In principle, the shape of the plot of  $c/I(\vartheta)$  against  $\sin^2\vartheta/2$  should furnish the dispersion, but in practice it seems hopeless to obtain data of sufficient precision to yield information on this point in any but extreme cases. Fortunately, the converse is also true; it is not necessary to have an accurate value of the dispersion in order to obtain  $b$  reasonably well from the data.

In this paper  $\langle \Delta n^2 \rangle$  will be estimated from the mode of preparation of the material. It will be assumed that the distribution of the original polymer is given by (13) with  $z=1$ . Using the solubility theory of Scott<sup>19</sup> distributions corresponding to the fractions prepared from the original material will be calculated. From these  $\langle \Delta n^2 \rangle$  will be found numerically.

To anticipate some of the results, it seems that  $z=19$  ( $\langle \Delta n^2 \rangle / \langle n \rangle^2 = 0.05$ ) corresponds fairly well to fractions prepared by several precipitations from dilute solution, if only a small part (e.g. ten percent) of the original material appears in the fraction in question. On the other hand,  $z=4$  ( $\langle \Delta n^2 \rangle / \langle n \rangle^2 = 0.20$ ) would seem to correspond to a crude fraction containing approximately one-fourth of the original material and prepared by a single precipitation.

To summarize, the dispersion,  $\langle \Delta n^2 \rangle$ , of the distribution should be estimated. From a plot of the limit of  $c/I(\vartheta)$  at infinite dilution against  $\sin^2(\vartheta/2)$ , by taking the ratio of the initial slope to the intercept, the quantity  $8\pi^2\langle n \rangle b^2(1 + \langle \Delta n^2 \rangle / \langle n \rangle^2) / 3\lambda^2$  may be found. A more accurate slope may be obtained by using the provisional slope and the dispersion in conjunction with Table II to rectify the plot. The quantity  $\langle n \rangle b^2 = L^2$  is the weight average of the mean square distance between the ends of the chains, while  $\langle n \rangle b^2(1 + \langle \Delta n^2 \rangle / \langle n \rangle^2)$  is the "Z-average" of the same quantity.

### 3. The Extrapolation to Infinite Dilution

Equation (1) shows that  $c/I$  is a linear function of  $c$  at low concentrations. We have just seen that it is also approximately a linear function of  $\sin^2(\vartheta/2)$ . Consequently, a bilinear method of plotting the data is indicated.

The procedure used in this work has been to plot  $c/I$  against  $\sin^2(\vartheta/2) + k'c$ , where  $k'$  is an arbitrary constant (e.g.,  $k'=100, 2, \frac{1}{2}$ , etc.) chosen for convenience. The data then fall on patterns such as are illustrated in Figs. 8 and 9. Lines may be drawn through points of the same value of  $\sin^2(\vartheta/2)$  to extrapolate to infinite dilution.

The characteristic patterns seen in Figs. 8 and 9 may be thought of as projections of the reciprocal intensity surface,<sup>5</sup> on a plane containing the

<sup>19</sup> R. L. Scott, J. Chem. Phys. 13, 178 (1945).

$c/I$  axis and forming an acute angle with both the  $c=0$  and  $\vartheta=0$  coordinate planes.

For some materials, especially those of very high molecular weight, a difficulty arises when terms in higher powers of the concentration become important, giving appreciable curvature to the lines. Theory indicates that the curvature should increase with both  $A_2$  and with  $M$ . Consequently, as the molecular weight goes up, it becomes necessary to measure points at lower concentrations to obtain a linear extrapolation. Examples are to be found in the data which follow.

It should also be noted that the derivation of Eq. (1) is not rigorous when  $A_2$  or  $M$  are too high. An apparent dependence of  $A_2$  on  $\vartheta$  might result in such a case.

#### IV. EXPERIMENTAL DETAILS AND RESULTS

##### 1. Materials

Two samples of polystyrene were used in this work. The first, designated by the code letters RT-H, was the same material measured previously and reported in an earlier paper.<sup>6</sup> It was prepared in the following manner: The monomer was washed with alkali to remove inhibitors, distilled at 15 mm, then allowed to stand six months at room temperature. The polymer was precipitated by pouring the one-third-polymerized mixture into alcohol. A broad fraction was obtained by precipitating about one-fourth of the sample from a one percent solution in butanone with methanol.

An attempt was made to calculate the dispersion of the molecular weight distribution of fraction RT-H, using the theory as developed by Scott.<sup>19</sup> The distribution function of the original polymer was assumed to be given by Eq. (9) with  $z=1$ . The various parameters of Scott's equations were adjusted so that the concentration and weight of the precipitate agreed with the actual values, and the distribution curve of the precipitate calculated. The ratio of the dispersion to the square of the mean degree of polymerization  $\langle \Delta n^2 \rangle / \langle n \rangle^2$ , was then calculated numerically from the distribution curve. The result was  $\langle \Delta n^2 \rangle / \langle n \rangle^2 = 0.2$ .

The other sample of polystyrene, for which the code EP-2 is used, was prepared by fractionation

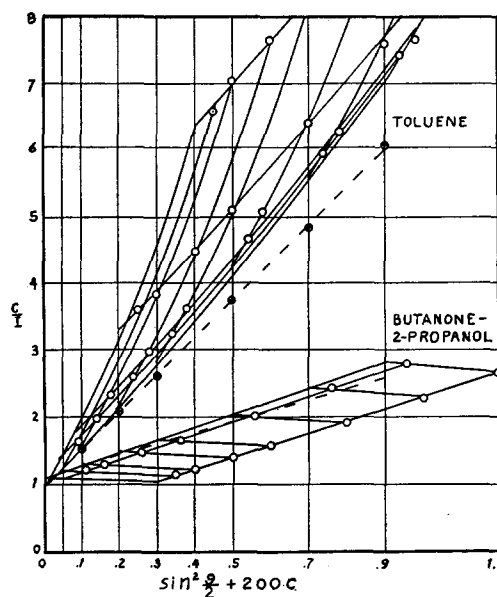


FIG. 9. Projection of the reciprocal intensity surfaces of polystyrene RT-H in toluene and in a butanone (89 percent), 2-propanol (11 percent) mixture at 20°C. The dotted lines are the limiting tangents. The toluene values have been divided by 3.54 (the theoretical ratio of the intercepts).

from an emulsion polymer, kindly supplied the author by Dr. A. Goldberg of the Polytechnic Institute of Brooklyn. The polymer had been prepared using ammonium stearate as suspending agent and persulfate ion as catalyst, in the same manner as described by Goldberg, Badgely and Mark.<sup>20</sup> The fractionation of this polymer was carried only far enough to yield a small fraction from the higher end of the distribution curve. The fraction was reprecipitated from dilute solution, yielding EP-2. Calculation by Scott's method, as described above, gave  $\langle \Delta n^2 \rangle / \langle n \rangle^2 = 0.05$ .

No extensive attempt was made to obtain chemically pure solvents, since only the relative solvent power was of interest. The benzene and toluene used were Baker and Adamson's "reagent," meeting A.C.S. specifications. The 1,2-dichloroethane was a commercial compound but the boiling point was 83.6° (corr.) (literature, 83.5°–7°). The butanone was first dried with  $\text{CaCl}_2$  to remove a considerable amount of water and alcohol and was then distilled, b.p. 79.5° (corr.) (lit. 79.6°). The isopropanol was not investigated.

<sup>20</sup> A. I. Goldberg, W. P. Hohenstein, and H. Mark, *J. Polymer Sci.* 2, 503 (1947).

TABLE III. Polystyrene EP-2 in butanone at 67°C.

Concentration (g/ml):		0.0019		0.00038	
$\vartheta$	$\sin^2(\vartheta/2)$	$I$	$(c/I) \times 10^5$	$I$	$(c/I) \times 10^5$
25.8°	0.050	—	—	7.38	5.13
36.9	0.100	29.8	6.36	7.34	5.18
53.0	0.200	28.5	6.66	6.96	5.45
66.4	0.300	27.9	6.84	6.78	5.61
90.0	0.500	26.2	7.27	6.29	6.02
113.6	0.700	24.7	7.70	5.88	6.47
143.1	0.900	23.5	8.10	5.54	6.84

$\lim_{c \rightarrow 0, \vartheta \rightarrow 0} c/I = 4.72 \times 10^{-5}$ .

## 2. Preparation of Solutions

A problem unique to light scattering is the removal of dust and foreign suspended matter from the solutions.

A bacterial filter of the Seitz type was found useful for some solutions if the asbestos pad was impregnated with Bakelite varnish and cured by baking. Without the treatment asbestos fibers were introduced in the solutions. Such filters seemed to remove particles larger than a few microns in diameter.

In some cases, however, suspended matter persisted even after this treatment, as shown by an excessive scattering at low angles from the solution. The solutions were then centrifuged at 15,000 times gravity for thirty minutes in a high-speed angle-head centrifuge, with marked improvement in the results.

The solvents were distilled in a small all-glass still with a sealed condenser just before use.

It was found that dilutions of the centrifuged solution could be made with distilled solvent and introduced into the measuring cell without the introduction of noticeable dust if all bottles, pipettes, etc. were carefully cleaned and rinsed with distilled solvent immediately before use.

It may be remarked that considerably more care in cleaning the solutions is required if angular dependence measurements are to be made than if only the transverse scattering alone is measured, as a result of the great dissymmetry of the radiation envelope of the dust particles. The scattering from the sulfur sol shown in Fig. 6 is typical, except for details, of that from other compact particles in the micron size range.

TABLE IV. Polystyrene RT-H in butanone (89 percent)-2-propanol (11 percent) at 20°C.

Concentration (g/ml):		0.00148		0.000296	
$\vartheta$	$\sin^2(\vartheta/2)$	$I$	$(c/I) \times 10^5$	$I$	$(c/I) \times 10^5$
25.8°	0.050	129.0	1.14	24.5	1.21
36.9	0.100	120.0	1.23	23.1	1.28
53.0	0.200	106.0	1.40	20.2	1.47
66.4	0.300	93.5	1.58	18.0	1.65
90.0	0.500	77.2	1.92	14.7	2.02
113.6	0.700	65.2	2.27	12.2	2.43
143.1	0.900	55.1	2.69	10.5	2.81

$\lim_{c \rightarrow 0, \vartheta \rightarrow 0} c/I = 1.11 \times 10^{-5}$ .

## 3. Procedure

Solutions, cleaned as described above, were introduced into the conical scattering cell and the intensities scattered at several angles in the, horizontal plane were measured. The incident light was vertically polarized and consisted of the 5461A line of the mercury spectrum plus some continuum for several hundred Angstrom units on either side of the line. Its mean wave-length was taken as 5460A.

Drifts of the voltage supply were checked by measuring the turbid polymer block (Section II, 8)

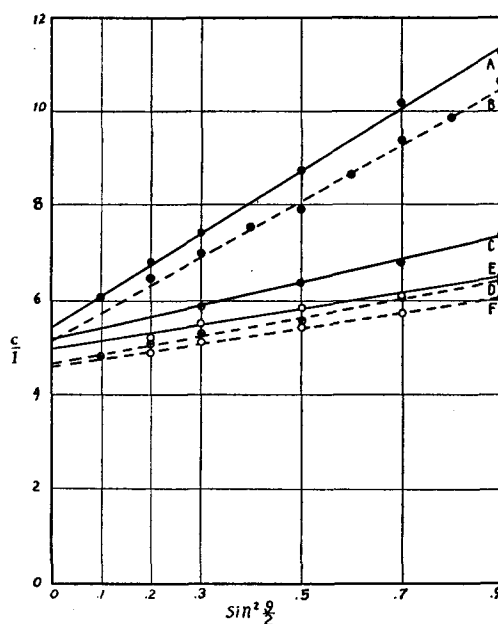


FIG. 10. Limiting tangents for polystyrene EP-2.

- A, toluene, 20°C, divided by 3.54
- B, toluene, 67°C, divided by 3.23
- C, butanone, 20°C
- D, butanone, 67°C
- E, butanone (87 percent), 2-propanol (13 percent), 20°C
- F, butanone (87 percent), 2-propanol (13 percent), 67°C

immediately before and after a series of measurements.

The determination of relative, not absolute, intensities was the primary aim of these experiments. However, the relative intensity scattered transversely from some of the solutions was compared to that from benzene. If previous measurements of the absolute scattering power of benzene are valid,<sup>21</sup> the absolute scattering of these solutions may be found. The comparison was made in rectangular cells giving negligible background scattering. Unpolarized light was used in this case. Since the depolarization of the excess light scattered from such solutions is very small,<sup>22</sup> there should be negligible change in the intensity of the excess transverse scattering in going to unpolarized illumination.

In order to get the temperature dependence of the scattering most accurately, the same samples of solution were measured at 20°C and 67°C in succession without refilling the cell.

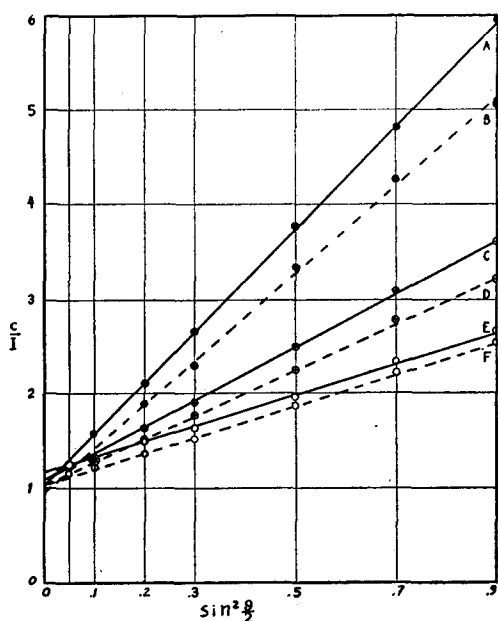


FIG. 11. Limiting tangents for polystyrene RT-H.

- A, toluene, 20°C, divided by 3.54
- B, toluene, 67°C, divided by 3.23
- C, butanone, 20°C
- D, butanone, 67°C
- E, butanone (89 percent), 2-propanol (11 percent), 20°C
- F, butanone (89 percent), 2-propanol (11 percent), 67°C

<sup>21</sup> S. Bhagavantam, *Scattering of Light and the Raman Effect* (Chemical Publishing Company, Brooklyn, New York 1942).

<sup>22</sup> P. Doty and H. S. Kaufman, *J. Phys. Chem.* **49**, 583 (1945).

TABLE V. Polystyrene RT-H in toluene at 20°C.

Concentration (g/ml):	0.00200		0.00100		0.00040		0.00020	
	$\vartheta$	$\sin^2(\vartheta/2)$	$I$	$(c/I) \times 10^6$	$I$	$(c/I) \times 10^6$	$I$	$(c/I) \times 10^6$
25.8°	0.050		8.65	23.2	7.86	12.8	5.82	6.89
36.9	0.100		8.02	24.9	7.38	13.6	4.88	8.17
53.0	0.200		7.41	27.0	6.37	15.8	3.82	10.5
66.4	0.300		6.88	29.0	5.58	18.0	3.12	12.8
90.0	0.500		5.95	33.7	4.42	22.6	2.25	17.9
113.6	0.700		5.35	37.5	3.73	26.9	1.80	22.1
143.1	0.900		4.79	41.7	3.15	31.8	1.48	27.0
			lim $c/I = 3.47 \times 10^{-6}$				$c \rightarrow 0, \vartheta \rightarrow 0$	

Viscosities were measured in specially constructed Ostwald pipettes having a low rate of shear. Comparison of results in different pipettes showed no dependence on shear rate in the range used.

#### 4. Results

In Tables III-V are given the intensities of scattering of the polymers in some typical cases, relative to the transverse (90°) scattering from benzene illuminated with unpolarized light at 20°C. The polymer solutions were illuminated with polarized light, and only the excess scattering over that of the solvent is given in each case. Concentration is given in terms of grams of polymer per milliliter of solution at the temperature of measurement. A small correction for the geometry of the cell has been applied, as described in Section II, 8.

##### A. Form of Reciprocal Intensity Surface

Plots of the results are shown in Figs. 8-11. In Figs. 8 and 9 are shown the complete projections of the reciprocal intensity surface<sup>5</sup> for three systems, EP-2 in butanone at 67°C, and RT-H in toluene and a butanone-propanol mixture at 20°C. From the theoretical development of the preceding paper,<sup>5</sup> it is expected that the portion of the  $c/I$  surface near the origin should be nearly planar. When plotted as in Fig. 8, the curves of constant  $c$  and constant  $\vartheta$  should then form two sets of parallel lines in this region. The figure shows that the expectation is well borne out; the maximum deviation of the slopes is less than five percent.

The data on RT-H in toluene, shown in Fig. 9, cover a larger region of the  $c/I$  surface, since the molecules are relatively much larger than those

TABLE VI. Mean length,  $L$ , and related quantities of polystyrene EP-2.

Solvent	Temperature	$A_2M$	$L(\text{Å})$
Toluene	20°C	180±15	1285±5%
	67	180±25	1220±5%
Butanone	20	80±10	887±5%
	67	80±10	828±5%
Butanone (87%), 2-Propanol (13%)	20	-10±10	745±5%
	67	+10±10	764±5%

giving rise to Fig. 8. The curvature of the surface is clear in Fig. 9.

To obtain the limiting tangents to the surfaces in the  $\vartheta$ -plane, use is made of Table II (section III. 2). Equation (12) shows that the expression  $\langle n \rangle (1 + \langle \Delta n^2 \rangle / \langle n^2 \rangle) C b^2 / 3$  is the ratio of the initial slope to the intercept of the curve of  $c/I$  against  $\sin^2(\vartheta/2)$  at  $c=0$ . From values of the slope and intercept estimated from the curve, the above expression may be approximated. Values of  $\langle u \rangle = \langle n \rangle C b^2 \sin^2(\vartheta/2) / 3$  may then be calculated for each value of  $\sin^2(\vartheta/2)$ . The fourth column of Table II then gives the factor that yields the point on the limiting tangent line when multiplied into the corresponding value of  $c/I$ . When the limiting tangent has been drawn through the points located in this way, the slope and intercept are determinable with greater precision than before. The process of approximation may be repeated with the new values, if necessary.

The dotted lines in Figs. 8 and 9 are the limiting tangents calculated as above. It is evident, especially in Fig. 9, that their use aids materially in determining the initial slopes.

In Fig. 9 some deviations from parallelism in the families of curves are noticeable at the larger values of  $\sin^2(\vartheta/2)$ . The effect may represent the beginning of a failure of the "single-contact" approximation of the preceding paper.

### B. The R.M.S. Chain Length

The data are apparently represented by Eq. (1) rather well. To save space, the complete reciprocal intensity surfaces are not shown for all the systems, but the tangent lines are reproduced in Figs. 10 and 11. From these  $(b^2 \langle n \rangle)^{1/2} = L$ , the weight-average root-mean-square end-to-end chain distance, may be calculated according to Eqs. (12) and (3). The results are shown in Tables VI and VII.

TABLE VII. Mean length,  $L$ , and related quantities of polystyrene RT-H.

Solvent	Temperature	$A_2M$	$L(\text{Å})$	$[\eta]$ (ml/g)	$L^3/[\eta]$
Toluene	20°C	930±70	2680±5%	767±15	2.5±15%×10 <sup>13</sup>
	67	690±70	2520±5%	742±15	2.3±15%×10 <sup>13</sup>
Butanone	20	300±30	1935±5%	315±10	2.2±15%×10 <sup>13</sup>
	67	300±30	1900±5%	261±10	2.6±15%×10 <sup>13</sup>
Butanone (89%), 2-Propanol (11%)	20	-100±30	1490±5%	—	—
	67	+90±30	1585±5%	—	—

Also shown in Tables VI and VII are some intrinsic viscosities and the values of the product  $A_2M$  which may be evaluated with the aid of Eq. (1) from the data. The quantity  $A_2$  is a measure of the deviation of the solution from Van't Hoff's law for the osmotic pressure and is therefore a measure of solvent power.<sup>23</sup> Large values of  $A_2$  occur with "good" solvents and small or negative values with "poor" solvents (in the thermodynamic sense). Since  $M$  is constant for the same material in different solvents,  $A_2M$  also serves as a relative measure of solvent power.

It is at once evident that there is a large change in the molecular extension, as measured by the mean length,  $L$ , when the solvent power is changed at constant temperature. Toluene is one of the best solvents for polystyrene known while the butanone-propanol mixture is near the precipitation point.

Parallel to the change in  $L$  goes a change in intrinsic viscosity. The data show that the intrinsic viscosity varies as the cube of  $L$ , as might be expected for large coiled molecules of this type.

These conclusions are qualitatively similar to those reached from earlier experiments on fraction RT-H,<sup>6</sup> but quantitatively the changes with solvent are much more pronounced. The discrepancy in the butanone value is especially large. The inaccuracy is felt to lie in the older experiments, which were done with comparatively crude apparatus and evaluated without theoretical refinements. The new viscosity determinations agree well with the old ones, indicating that the sample had not changed during the two years that elapsed between measurements. However, the extrapolation of the old data has had to be revised in the light of the new measurements,

<sup>23</sup> B. Zimm, J. Chem. Phys. 14, 164 (1946).



TABLE VIII. Molecular weight,  $M$ , characteristic length,  $b$ , and related quantities of polystyrene EP-2.

Solvent	Temperature	$[I_v]$	$\partial\mu/\partial c$	$M$	$b(A)$	$\cos\varphi$
Toluene	20°C	0.067	0.108	696,000	11.3	0.930
	67				10.8	0.922
Butanone	20	0.251	0.221	732,000	7.85	0.855
	67				7.30	0.835
Butanone (87%), 2-Propanol (13%)	20	0.264	0.221	771,000	6.58	0.800
	67				6.76	0.810
				Average 733,000		

giving more weight to the points at low concentrations.

### C. The Effect of Temperature

The effect of temperature on the mean extension,  $L$ , is noteworthy. In considering the phenomena, it must be borne in mind that the molecules are considerably more extended than would be the case if there were free rotation about the bonds of the chain skeleton, as is shown in section  $D$ , below. In toluene, a good solvent, there is apparently only a very slight tendency for the molecule to curl up and become smaller as the temperature rises. This would seem to indicate that the chain is extended by energies considerably larger than the average thermal agitation energy, as measured by  $kT$ , which most probably result from some kind of steric hindrance between the segments. If the large extension were the result of a normal ( $\sim 4000$  cal.) barrier to rotation about the single bonds of the chain skeleton, as calculated by Taylor<sup>24</sup> for paraffins, the temperature coefficient of  $L$  would be much larger than actually found.

In the butanone-propanol mixtures, which are very poor solvents, an *increase* of the mean extension with increase of temperature is noted. It would seem that the presence of a poor solvent gives rise to attractive forces between the chain segments, the energies associated with these forces being of the same order as  $kT$  so that a large temperature coefficient results. The energies also cause the chain to favor the more highly curled configurations giving rise to the observed small extensions in the poor solvent.

Another interesting effect appears in the change of the product  $A_2M$  with temperature, which reflects the variation of  $A_2$  alone, since pre-

<sup>24</sup> W. J. Taylor, J. Chem. Phys. 16, 257 (1948).

 TABLE IX. Molecular weight,  $M$ , characteristic length,  $b$ , and related quantities of polystyrene RT-H.

Solvent	Temperature	$[I_v]$	$\partial\mu/\partial c$	$M$	$b(A)$	$\cos\varphi$
Toluene	20°C	0.375	0.108	3,890,000	10.7	0.919
	67				10.1	0.908
Butanone	20	1.17	0.221	3,420,000	7.68	0.848
	67				7.58	0.837
Butanone (89%), 2-Propanol (11%)	20	1.17	0.221	3,420,000	5.95	0.760
	67				6.32	0.785
				Average 3,580,000		

sumably  $M$  does not change. (The change of intercept with temperature in Figs. 10 and 11 can be explained as the result in changes of the refractive indices.) It has been shown previously<sup>23</sup> that the heat of dilution of the system,  $\Delta\bar{H}_1$ , is related to  $A_2$  in dilute solutions by the equation,

$$\Delta\bar{H}_1 = -R(\partial(A_2/V_1)/\partial(1/T))V_1^2c^2, \quad (18)$$

where  $R$  is the molar gas constant and  $V_1$  is the volume of the solvent per mole. Since  $V_1$  increases by nearly five percent when the temperature changes from 20°C to 67°C, while  $A_2$  either does not change or decreases slightly in toluene,  $\Delta\bar{H}_1$  must be negative in this system (i.e., heat is evolved on dilution).<sup>25</sup>

Negative heats of dilution are not commonly observed in hydrocarbon mixtures. While it is not appropriate here to discuss exhaustively possible explanations, the two following seem likely: (a) It has been shown that  $A_2$  decreases as the extension of the molecule decreases,<sup>23</sup> and a small decrease with increasing temperature seems possible in view of the data in Tables XVII and XVIII. (b) It is well known that the thermal expansion coefficient of the polymer is less than that of the common solvents. Since  $A_2$  is of the nature of an excluded volume of a polymer molecule, it would not be expected to increase as fast with temperature as the molar volume,  $V_1$ , of an indifferent solvent. Cooperation of the two effects could explain the observations. It may be noted that both are peculiar to macromolecular solutions.

In the poor solvent, the butanone-propanol mixture,  $A_2$  increases with temperature, corresponding to a positive heat of mixing, as expected.

Pure butanone seems to be an intermediate case.

<sup>25</sup> Professor P. M. Doty has informed me that he has observed the same effect in osmotic measurements on this system.

### D. Determination of Molecular Weight

The molecular weight of the samples may be found if the ratio of the intensity of scattering to the incident intensity can be evaluated. The absolute scattering power of benzene has been reported by two authors.<sup>26,27</sup> Their results give the quantity  $i_{90}r^2/I_u^0$ , where  $i_{90}$  is the intensity scattered at  $90^\circ$  at a distance  $r$  from a cubic centimeter of liquid, and  $I_u^0$  is the intensity of the unpolarized incident beam. For the discussion, we shall define the following terms:

$I(\vartheta)$ , the *relative intensity*, expressed in terms of some convenient quantity (in this paper the transverse scattering from the same volume of benzene at the same distance, the benzene being under unpolarized illumination),

$I_{\vartheta u} = i_{\vartheta}r^2/I_u^0$ , the *reduced intensity* with unpolarized illumination,

$I_{\vartheta v} = i_{\vartheta}r^2/I_v^0$ , the *reduced intensity* with vertically polarized illumination, and

$\tau = 2\pi \int_0^\pi I_{\vartheta u} \sin\vartheta d\vartheta$ , the *turbidity*, equal to the total scattering per centimeter of path (polarization of incident light immaterial).

In addition, the term *reciprocal scattering function* has already been used for the quantity  $c/I(\vartheta)$ .

A well-known formula relates the reciprocal of the limit of  $c/I_{\vartheta v}$  as  $c$  and  $\vartheta$  approach zero to the weight-average molecular weight  $\langle M \rangle$ . The relation follows, with  $\mu$  the refractive index of the solution and  $\lambda_0$  the wave-length *in vacuo*:

$$\lim_{c \rightarrow 0, \vartheta \rightarrow 0} \frac{I_{\vartheta v}}{c} \equiv [I_v] = \frac{4\pi^2 \mu^2 (\partial\mu/\partial c)^2}{\lambda_0^4 N_0} \langle M \rangle, \quad (19)$$

$$= K \langle M \rangle.$$

The term *intrinsic scattering* (either relative or reduced), with the symbol  $[I]$ , might be proposed for the important quantity  $\lim I/c$ .

Cabannes and Daure<sup>26</sup> report a value of  $10.7 \times 10^{-6}$  for the reduced intensity  $I_{90u}$ , with an average wave-length in vacuum,  $\lambda_0$ , of 5440Å and at a temperature of  $15^\circ\text{C}$ . Peyrot<sup>27</sup> reports  $34.8 \times 10^{-6}$  for the same quantity with 4358Å light at  $25^\circ\text{C}$ . From these we estimate a value of  $13 \times 10^{-6}$  for  $I_{90u}$  for benzene at  $20^\circ\text{C}$  with light of 5460Å. Multiplication of the relative intensities by  $13 \times 10^{-6}$  then leads to the reduced

<sup>26</sup> J. Cabannes and Daure, *Comptes rendus* **184**, 520 (1927).

<sup>27</sup> P. Peyrot, *Comptes rendus* **203**, 1512 (1936).

intensities, from which the molecular weight is obtained by Eq. (19).

The results are given in Tables VIII and IX, together with the values of  $\partial\mu/\partial c$  which were used in the calculation. The latter quantities were estimated from several previous determinations.<sup>28</sup> It may be noted that the determinations in different solvents agree tolerably well.

Also in Tables VIII and IX are the results for  $\cos\varphi$ , the average of the cosine of the angle of rotation of the carbon atoms about the bonds joining them in the chain, calculated from Taylor's<sup>24</sup> formula,

$$L^2 = \sigma^2 \left( \frac{1 + \cos\alpha}{1 - \cos\alpha} \right) \left( \frac{1 + \cos\varphi}{1 - \cos\varphi} \right) (2\langle n \rangle), \quad (20)$$

$$= b^2 \langle n \rangle,$$

where  $\sigma$  is the length of a single bond (1.55Å) and  $\alpha$  the bond angle ( $70.5^\circ$ ). It can be seen that  $\cos\varphi$  is the same for the two materials in any given solvent, which seems to show that the microstructure of the different polymers is the same. It is also important that  $\cos\varphi$  is much greater than zero in all cases, showing that rotation about the chain bonds is not free.<sup>29</sup>

### V. CONCLUSION

The data that have been quoted in the preceding section seem to show that the combined theoretical and experimental techniques of light scattering are sufficiently developed to yield important results concerning the extension of macromolecular chains. As more data, especially on temperature dependence, become available, it may be possible to theorize with some confidence concerning the intramolecular energies that determine the shape and size of such complicated structures as the polystyrene molecule. The results of this investigation at least encourage such a hope.

### ACKNOWLEDGMENT

It is a pleasure to acknowledge the help of Mr. C. I. Carr in construction of the apparatus.

<sup>28</sup> P. M. Doty, B. H. Zimm and H. Mark, *J. Chem. Phys.* **12**, 144 (1944); also unpublished data of the author's.

<sup>29</sup> Comparison of these molecular weights with previous osmotic determinations on similar materials makes the values in Table XIX seem surprisingly low. A critical study of the reduced intensity determination has therefore been started. Pending further results, these molecular weights should be considered as provisional values.